BELLCOMM, INC.
955 L'ENFANT PLAZA NORTH, S.W., WASHINGTON, D.C. 20024

COVER SHEET FOR TECHNICAL MEMORANDUM

TITLE- Support Motion Induced Vibrations of an Orbiting Cassegrain Telescope

TM- 70-1022-3

DATE- March 17, 1970

FILING CASE NO(S)- 620

AUTHOR(S)- P. G. Smith

FILING SUBJECT(S) (ASSIGNED BY AUTHOR(S))- Space Astronomy
Telescope Deflection
Gimbal Mounted Space Telescopes
Effects of Astronaut Motion

ABSTRACT

A structural model of a Cassegrain space telescope is developed to determine structural deformation and associated optical degradation resulting from motions of a supporting spacecraft. Three specific designs, a 1 meter f-30, a 1 meter f-60, and a 2 meter f-60, are investigated using the model, which represents the basic structure, mirrors, detailed mirror mountings, and an experiment package. All three designs retain their diffraction-limited performance when excited by deterministic representations of astronaut motion disturbances or by worst case control system disturbances. Special attention is given to the coordinates used in order to obtain good numerical accuracy. Also, a means for determining the amount of error in the results is presented.

Further investigation is suggested to determine the deformation due to random crew motion representations as well as the effect of the telescope attitude control system on deformation.

TABLE OF CONTENTS

BELLCOMM, INC.
955 L'ENFANT PLAZA NORTH, S.W. WASHINGTON, D. C. 20024

SUBJECT: Support Motion Induced Vibrations of an Orbiting Cassegrain Telescope Case 620

DATE: March 17, 1970

FROM: P. G. Smith

TM-70-1022-3

TECHNICAL MEMORANDUM

1.0 INTRODUCTION AND RELATED WORK

1.1 Introduction

Many benefits arise from having men aboard an Earth orbital astronomical facility [1],* but attendant with a crew are certain technical problems whose impact on operation of the facility must be assessed. One such problem is the transmission of crew-induced spacecraft motion to the astronomical instruments, and consequently the writer [2] and others [3,4,5] have reported on gross motions of an experiment package due to crew motion.

In this memorandum the crew motion induced vibrations of individual optical elements are examined. Such vibrations of specific elements are of particular concern for a gimbal mounted** experiment package, for although gimbals provide rotational isolation, they do not protect the instruments from translational disturbances. It is the purpose of this memorandum to determine how the performance of a gimbal mounted Cassegrain telescope might be limited by motion of individual optical elements resulting from translational disturbances or from control torques applied about the gimbal axes. This is done by determining the response of optical elements in analytical models of certain specific telescopes to representations of the disturbances just mentioned: if, for a structure of reasonable weight, the optical element responses fall within predetermined tolerances for that telescope, then the use of a gimbal mounting is not precluded.

1.2 Related Work

A study somewhat similar to this one was performed for a 26 inch photoheliograph at Jet Propulsion Laboratory [7]. The major differences are that the excitation in that case is

---

*Numbers in brackets designate References at the end of the memorandum.

**See Reference 6 for a description of the type of gimbal mount under discussion.

seismic rather than due to crew motion disturbances, and the performance criterion there is a change in total pathlength rather than amplitude of optical element motion.

G. M. Anderson [8] has studied the deflection of a telescope due to crew motion. His model is simpler than the one used here, but this simplicity allows him to present his results in terms of three nondimensional parameters so that general conclusions can be drawn. In particular, he demonstrates the advantage of very compliant* support springs.

Due to the structural design of the Apollo Telescope Mount (ATM) Experiment Package, it has been sufficient to perform a modal analysis of the cruciform-shaped spar (the main structural member) [9], define excitations acting on the spar, and provide each experiment designer with the resulting responses at the base of his experiment. These responses - considered as excitations by the experiment designers - have been used to find responses of critical experiment components, such as the primary mirror and gimbal assembly in the S055 scanning spectrometer. [10]

2.0 STRUCTURAL MODEL

2.1 The Structure

We consider a pin-connected, three-dimensional truss structure having the general shape of a regular hexagonal prism, as shown in Figure 2.1. In this figure $A_{i,j}$, $C_{i,j}$, and $D_{i,j}$ respectively denote axial, circumferential, and diagonal members; the first subscript, denoted by i in general, i=1,...,6, indicates locations around the hexagon, and the second subscript, denoted by j, j=1,..., r, indicates locations along the structure, starting at the front.

Inasmuch as the vertices of the hexagons are assumed to be pin-connected, one can see that the structure shown in Figure 2.1 is incompletely constrained, that is, it is incapable of supporting loads in the planes of the hexagons. The required constraint is introduced by adding members connecting alternate corners of each hexagon, as shown in Figure 2.2. Six of these members, called braces and denoted by $B_{i,j}$, are provided for each hexagon; it is important that they do not pass through the hexagon.**

---

*That is, natural frequency near orbital frequency.

**The area inside the hexagon constitutes the barrel of the telescope, and it should not be obstructed.

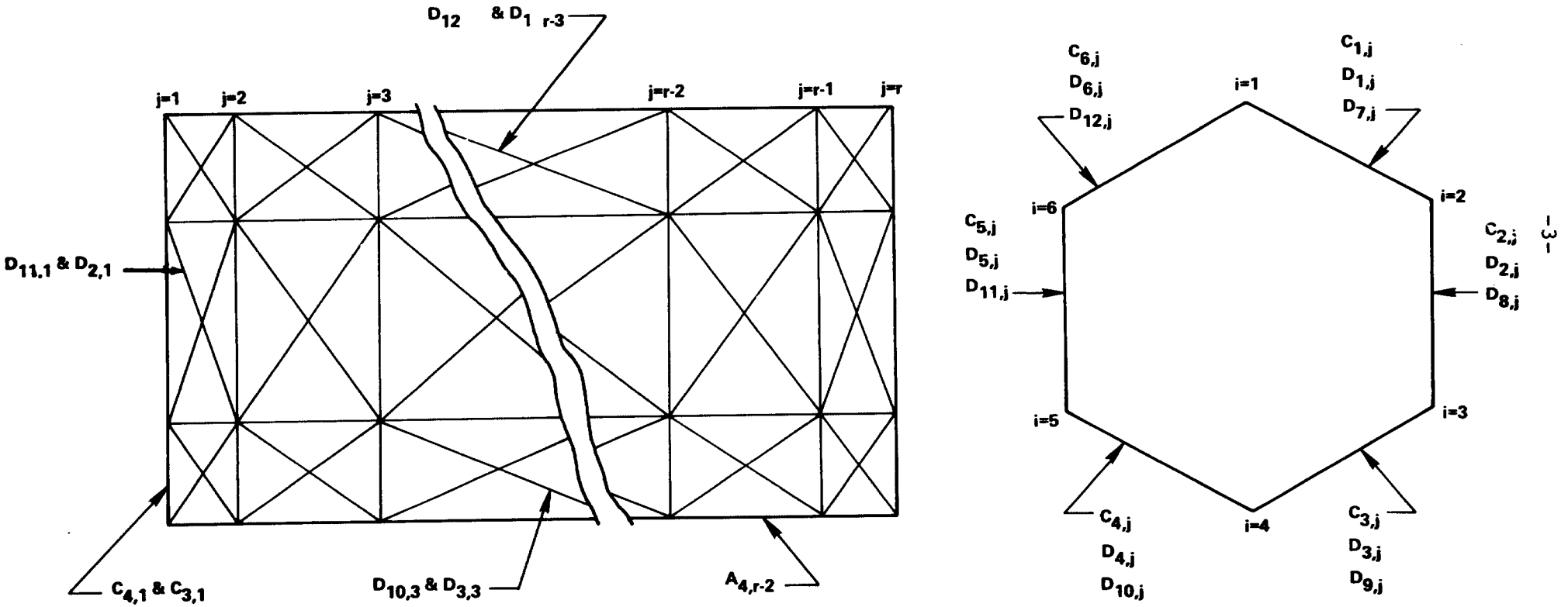

Figure 2.1
Hexagonal truss structure

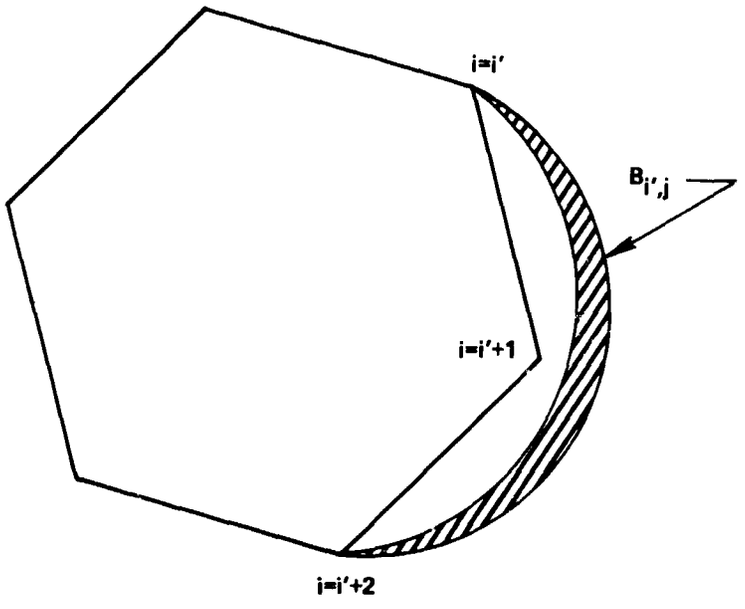

Figure 2.2
A typical brace

The primary mirror is attached to hexagons r-1 and r by means of the three primary mirror supports illustrated in Figure 2.3. The forward primary mirror supports, denoted by F_i, lie in the plane of the r-1 hexagon, and in addition there are aft primary mirror supports, denoted by G_i.* The mirror is mounted to the ends of the three supports by means of tangent bars similar to those used in the Goddard Experiment Package [11]; although the bars are assumed to be rigid in the direction of the telescope axis, distinct compliances are provided for each bar in both the radial and tangential directions.

---

*The naming convention for members, for example, A for axial, breaks down after the letter F.

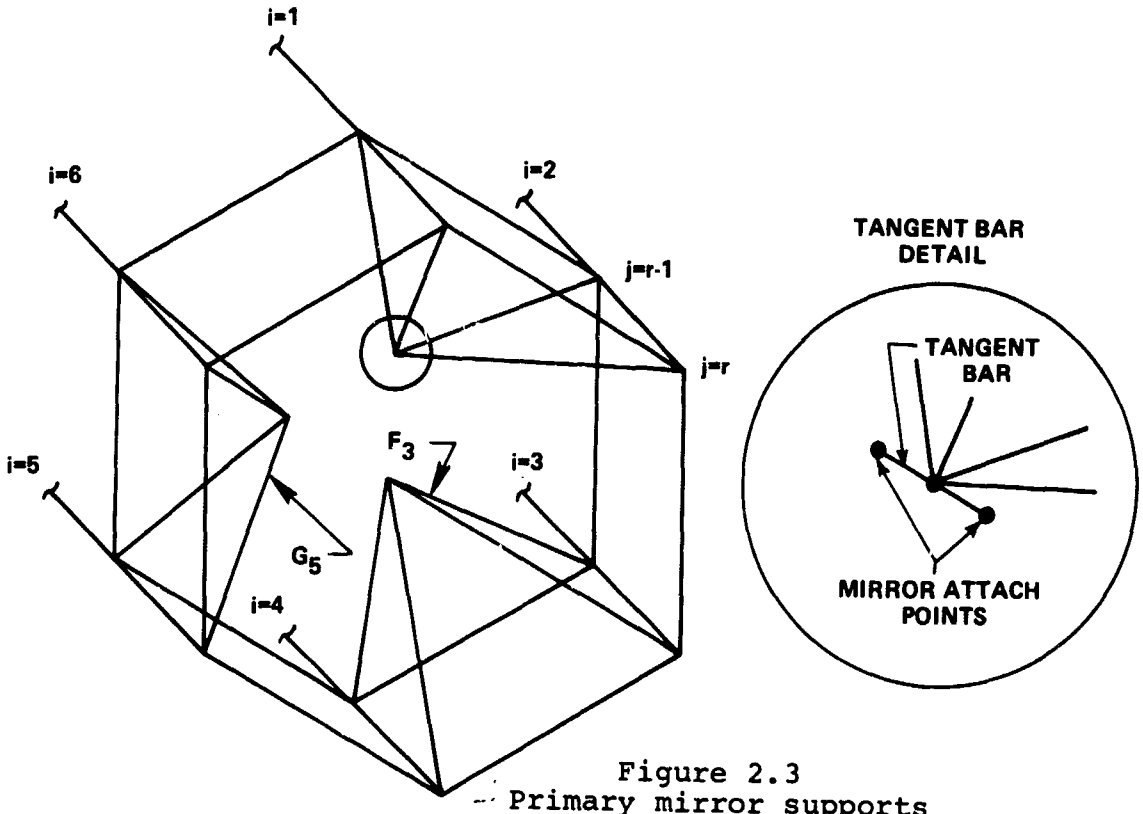

Figure 2.3
Primary mirror supports
(Diagonals and braces omitted for clarity.)

The secondary mirror is attached to the first two hexagons, as shown in Figure 2.4, by means of six secondary mirror supports, denoted by H_i. Again we notice that because of the pin-connected assumption, the mirror is unconstrained in rotation about the axial direction; however, constraint may be provided by simply pretensioning the secondary mirror supports, the amount of pretension in each H_i being denoted by h.

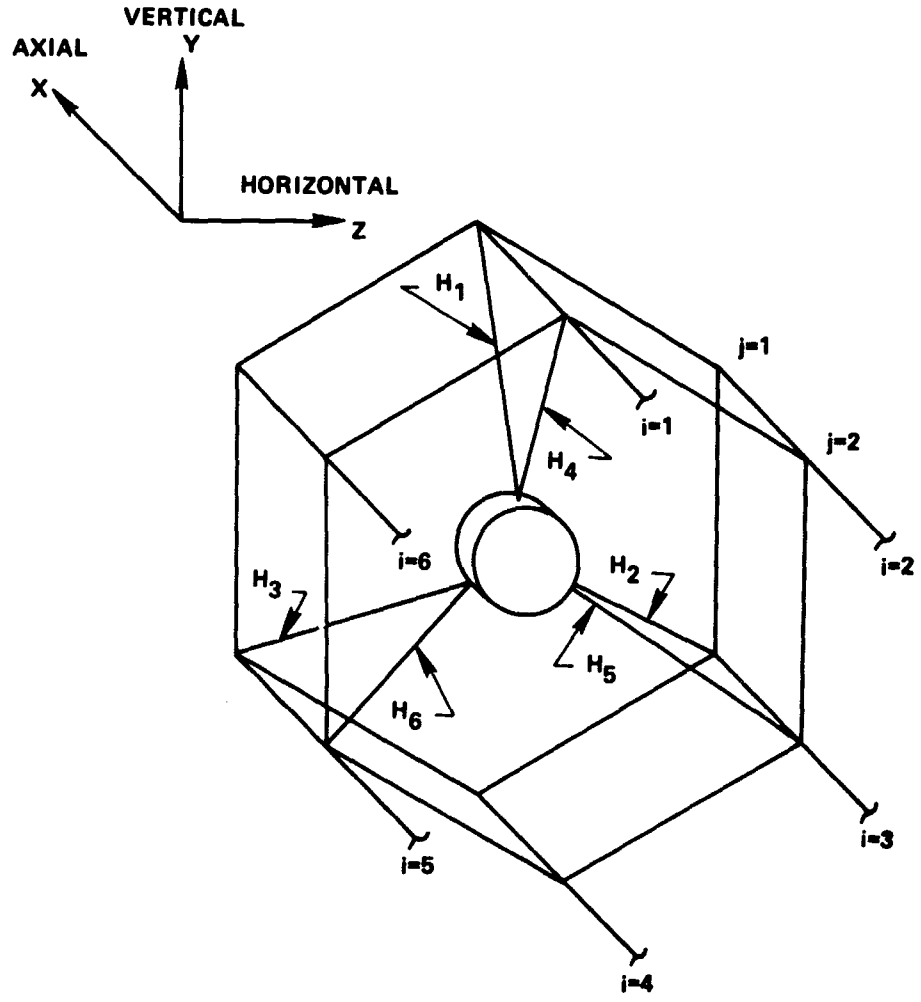

Figure 2.4
Secondary mirror and supports
(Diagonals and braces omitted for clarity.)

The experiments, which are considered as a point mass, are attached to the aft hexagon (j=r) by means of six experiment supports, denoted by E_i; see Figure 2.5.

The telescope structure is attached to the spacecraft by means of support springs connecting one of the hexagons, denoted hexagon j=s, to the attitude control gimbals.

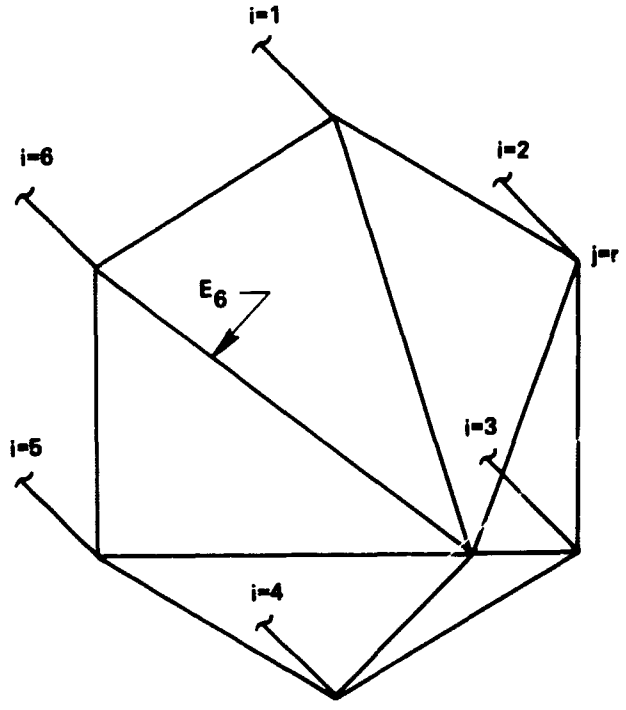

Figure 2.5
Experiment supports
(Diagonals and braces omitted for clarity.)

The x, y, and z axes shown in Figure 2.4 establish three mutually orthogonal directions that we shall call the axial, vertical, and horizontal directions, respectively.

2.2 Criteria for Choosing the Structure

The structure just described is chosen to show how the elements of a Cassegrain telescope may be mounted so as not to be excessively displaced when the telescope is subjected to loads arising because of the gimbal mounting.

Since motions of optical elements in an actual telescope may be highly dependent on telescope mass distribution and on mirror mounting details, consideration is given to modeling these items accurately with respect to an actual telescope structure. Moreover, to ensure that analytical results from the model correlate well with results for an actual structure, a structural model is chosen such that an actual structure can be reduced to the analytical model with a minimum of idealization and approximation.

Most likely there are structures that are in some sense better than the one described in Section 2.1. However, the objective of this work is not to find an optimal structure but rather to demonstrate rigorously that for the structure considered, crew motion induced optical element displacements are not excessive.

relative axial translation - that is, displacement of the secondary relative to the primary, parallel to the optical axis;

relative lateral translation - same as above except normal to the optical axis;

relative rotation - again, only rotation normal to the optical axis is considered.

Collectively, these are called the significant motions.

3.3 Obtaining Displacement from Excitation

Equations of motion for the structure are obtained in Appendix A, where they are also rendered into uncoupled form. One can obtain closed-form solutions to these uncoupled equations for each of the six periodic excitations discussed in Section 3.1. Structural damping is accounted for by adding a small amount of viscous damping (less than 5 percent of critical) to each of the uncoupled equations.

4.0 RESULTS

4.1 Introduction to the Numerical Investigation

Optically significant response motions are presented here for three specific telescope designs, namely, a 1 meter f-30 system, a 1 meter f-60 system, and a 2 meter f-60 system.* Compared to the 1 meter f-30 system, the 1 meter f-60 system shows the effect of increasing focal length so as to make the diffraction image comparable in size to the resolution of current image detectors. The 2 meter system then illustrates the effect of increased aperture. Table 4.1, prepared by D. B. Wood,** gives pertinent data for the three systems.

Data for the three final designs are given in Sections 4.2-4.4. Structural members for the 1 meter f-30 design are sized by making repeated modal analyses, each of which suggests structural changes that may result in lower deflection and/or weight when the next modal analysis is made. The other two designs are obtained directly from the 1 meter f-30 design, as described in Sections 4.3 and 4.4. A 500 lb experiment package is assigned to the 1 meter f-30 system, and the primary and secondary mirror weights of 320 lb and 25 lb, respectively, were suggested by B. W. Jackson of Kollsman Instrument Corporation. Invar is used for the structural material because of its desirable thermal expansion properties.

---

*These three systems were suggested by D. B. Wood.

**Mr. Wood will issue a memorandum on this work.

TABLE 4.1

Dimensions and Allowable Displacements

	1 meter, f-30	1 meter, f-60	2 meter, f-60
Aperture - in	39.4	39.4	78.8
Primary focal ratio	4.0	6.0	6.0
Secondary magnification	7.5	10.0	10.0
System focal ratio	30.0	60.0	60.0
Distance between mirrors - in	138.1	213.0	426.0
Distance from primary to focal point - in	7.9	19.7	39.4
Diameter of secondary - in	5.2	4.4	8.8
Allowable primary mirror rotation - rad	3.0×10^{-7}	3.0×10^{-7}	1.5×10^{-7}
Allowable relative axial translation* - in	1.5×10^{-3}	1.1×10^{-3}	1.1×10^{-3}
Allowable relative lateral translation* - in	1.4×10^{-4}	0.8×10^{-4}	0.8×10^{-4}
Allowable relative rotation* - rad	2×10^{-6}	3×10^{-6}	1.5×10^{-6}

*Based on the criterion that image motion or lack of focus shall be less than one-fourth the diameter of the central portion of the diffraction image at 5000 A.

The table may be interpreted by taking the largest value in a given column (1.6×10^{-9} in the first column) and comparing it with the associated allowable value from Table 4.1 (3.0×10^{-7}) to see if the response is acceptably small. Following this procedure, one finds that primary mirror rotation is 5.3×10^{-3} of the allowable, relative axial translation is 1.5×10^{-5} of the allowable, relative lateral translation is 6.6×10^{-4} of the allowable, and relative rotation is 1.6×10^{-3} of the allowable.

The numbers in Table 4.2 are the same for either no structural damping or one percent of critical damping. Furthermore, the results are essentially the same for excitation frequencies of 0.25 and 1.00 Hertz as they are for 0.5 Hertz.*

The 1 meter, f-30 telescope investigated weighs 1130 lb, of which 850 lb is due to the mirrors and experiments.

4.3 1 Meter, f-60 Design

This design is the same as that specified in Appendix F except that distances between certain of the hexagons increase,** and consequently the support spring constants, $_{s}k_{i}$, decrease due to increased structural compliance at the supports. Table 4.3 illustrates the response of this design to the same periodic support displacement excitation used with the f-30 design.

Note that primary mirror rotation now rises to 2.8% of the allowable value and relative lateral translation becomes 1.1% of the allowable, although the other two responses remain well below one percent of their allowable values.

This telescope weights 1175 lb.

---

*The lowest frequency of the structure is 4.0 Hertz.

**Specifically, $\alpha_2 = \alpha_3 = 53.$, $\alpha_4 = 79.41$, and $\alpha_5 = 24.59$.

TABLE 4.3

Response Data for the 1 Meter, f-60 Design

Response / Excitation	Prim. mirror rotation (rad)	Rel. axial translation (in)	Rel. lateral translation (in)	Relative Rotation (rad)
Translation - axial	8.5×10^{-11}	2.3×10^{-8}	1.5×10^{-8}	9.9×10^{-12}
Translation - vertical	8.7×10^{-10}	4.7×10^{-9}	8.1×10^{-7}	7.8×10^{-10}
Translation - horizontal	6.0×10^{-10}	3.0×10^{-10}	8.5×10^{-7}	6.1×10^{-10}
Rotation - axial	1.4×10^{-11}	1.2×10^{-10}	8.2×10^{-10}	7.5×10^{-11}
Rotation - vertical	8.3×10^{-9}*	6.2×10^{-12}	1.1×10^{-7}	8.1×10^{-11}
Rotation - horizontal	7.8×10^{-9}*	2.1×10^{-10}	1.0×10^{-7}	6.9×10^{-11}

4.4 2 Meter, f-60 Design

Design values for this case are obtained from those for the 1 meter, f-60 design by applying the following scaling relationships.

Double all lengths.**

Double all cross-sectional areas--This maintains th the member stiffnesses.

Increase mirror masses eightfold - B. W. Jackson indicates that mirror mass varies approximately as aperture cubed.

---

*Total rotations are 3.1×10^{-8} and 3.0×10^{-8} rad, respectively.

**Except for α_4 and α_5, which must be recomputed to maintain telescope mass center at the support point.

Double experiment mass.

Maintain spring stiffness as before* - This is consistent with cross-sectional area scaling.

Table 4.4 shows the response of this design to the same excitation used previously.

TABLE 4.4

Response Data for the 2 Meter, f-60 Design

Response / Excitation	Prim. mirror rotation (rad)	Rel. axial translation (in)	Rel. lateral translation (in)	Relative Rotation (rad)
Translation - axial	2.5×10^{-10}	9.1×10^{-9}	7.3×10^{-8}	2.2×10^{-10}
Translation - vertical	2.2×10^{-9}	2.4×10^{-8}	3.4×10^{-6}	4.2×10^{-9}
Translation - horizontal	1.1×10^{-9}	4.5×10^{-9}	3.5×10^{-6}	3.8×10^{-9}
Rotation - axial	6.8×10^{-11}	4.4×10^{-10}	5.0×10^{-9}	3.6×10^{-10}
Rotation - vertical	3.6×10^{-8}**	1.2×10^{-10}	7.5×10^{-7}	3.6×10^{-10}
Rotation - horizontal	4.1×10^{-8}**	1.7×10^{-9}	8.4×10^{-7}	4.2×10^{-10}

*Support spring constants are recomputed, as discussed previously, but their values remain close to those for the 1 meter, f-60 design.

**Total rotations are 4.4×10^{-8} and 4.7×10^{-8} rad, respectively.

Comparison of the values from Table 4.4 with the allowables from Table 4.1 shows responses to be 0.27, 2.2×10^{-5}, .044, and .0028 of the respective allowables. At 1.0 Hertz excitation frequency, primary mirror rotation reduces to .073 of the allowable and the other significant motions remain virtually unchanged, even though the first three resonant frequencies of the structure are 1.07,* 1.33, and 1.35 Hertz.

The weight for this design is 5080 lb.

5.0 NUMERICAL ACCURACY

Considerable effort was expended in obtaining satisfactory accuracy in the results presented in Tables 4.2 - 4.4. One method of determining accuracy of the numerical results is given in Appendix G, where it is shown that error in the values given in Table 4.2 is on the order of 1% and error in Table 4.4 runs as high as 28%. Although 28% is more error than one would like to see, it is quite satisfactory for the present purpose.

6.0 CONCLUSIONS

6.1 Conclusions Drawn from this Work

For the crew motion and control system disturbances considered, we have shown that displacements** of a Cassegrain space telescope remain within the range allowable for diffraction-limited performance. Three specific designs are considered, two of them having one meter apertures and weighing about 1000 lb each,***and the third being a two meter, f-60 design weighing about 5000 lb.

Consider first the displacements due to crew motion disturbances. The highest ratio of computed displacement to allowable displacement is .0053 for the 1 meter f-30 design, .011 for the 1 meter f-60 design and .044 for the 2 meter f-60 design. On this basis, structural deformation due to crew motion is not a problem, and it should not be a problem even for much larger telescopes. However, calculations for a single

---

*The mode associated with 1.07 Hertz resonance does not contribute to the significant motions.

**Displacement denotes both translation and rotation.

***Includes weight of the structure, mirrors, and experiments.

degree of freedom system indicate that the sine wave crew motion disturbance used here yields smaller responses than random crew motion, which can excite the lightly damped low frequency telescope modes more effectively than a sine wave. Therefore, the small ratios given above might increase when random crew motion is used.

Displacements arising from worst case control system disturbances are essentially the same for the two 1 meter designs as they would be for a rigid telescope. The 2 meter design yields about 70 percent larger responses to control system disturbances than a corresponding rigid telescope. We conclude that response to control system disturbances cannot be reduced appreciably by stiffening the telescope structure.

A significant contribution of this work is in computing small structural displacements accurately when using a modal analysis for a large, complex structure. This is done by finding the proper set of coordinates and by devising a test for numerical accuracy.

The structural model developed here is quite detailed, and therefore the associated computer program is useful for other structural dynamic analyses of telescopes. Besides the work discussed in the next section, one could investigate with minimal modification responses due to such things as aperture door motion, film transport, and pump operation.

6.2 Future Work Required

Recent studies [14] show that crew motion is best represented as a random process, and therefore a final answer to the question of crew motion excited telescope vibrations awaits a random vibration study. Such a study should include such items as spacecraft and telescope resonant frequencies and structural damping, as well as both spacecraft and telescope attitude control systems. In fact, the telescope attitude control system is expected to play a large role in determining the vibrational response to random crew motion.

A study including all of the items just mentioned is in progress. Should that study show the structural designs presented herein to be unacceptable, it will be necessary to stiffen them appropriately. Only failing this will it be necessary to consider translational decoupling or image motion compensation as a means of obtaining satisfactory optical performance.

7.0 ACKNOWLEDGEMENT

Several people contributed substantially to this work, and I would like to take this opportunity to express my gratitude.

Fred Brewer and Pat Dowling wrote the computer program.

As previously mentioned, Dave Wood suggested both the type of telescope and the telescope sizes used in this study. He provided the essential dimensions, the allowable limits for mirror motion, and a few astronomy lessons for the author.

Bailey Jackson (Kollsman) contributed details on the mirror mountings and provided values for the mirror weights.

John Garba (JPL) and Shou-nien Hou contributed through discussions on analytical and numerical methods.

P. G. Smith

1022-PGS-mef

Attachments
References
Appendix A-G

APPENDIX A

Modal Analysis

Definition of Coordinates

The structure described in Section 2.1 has 18r+21 degrees of freedom of which 18r are associated with the basic hexagonal structure, 3 are associated with the experiments, 9 with the primary mirror supports, 3 with the primary mirror, and 6 with the secondary mirror. The corresponding coordinates are ordered as follows.

Basic hexagons: First is x direction translation for i=1, j=1; y and z translations for this point follow; next are x, y, z for i=2, j=1; etc.

Experiments: Coordinate 18r+1 is the x translation at the experiment location; y and z translations at this location follow.

Primary mirror supports: The x translation at the end of the first support (the one between i=1 and i=2; see Figure 2.3) is coordinate 18r+4; the y and z translations at this point follow; next are x, y, z for the support between i=3 and i=4, and then x, y, z for the third support.

Primary mirror: Coordinate 18r+13 is rotation of the mirror about x;* coordinates 18r+14 and 18r+15 are y and z translations of the center of the mirror.*

Secondary mirror: Coordinates 18r+16 through 18r+18 are x, y, z translations of the center of the mirror, and 18r+19 through 18r+21 are x, y, z rotations.

---

*Recall that the primary mirror is constrained not to move axially relative to its supports, so that relative to its supports it has only the three degrees of freedom mentioned.

Stiffness Matrix

A method for generating an (18r+21)x(18r+21) symmetric stiffness matrix, K, by the displacement method with a minimum of labor is now described. Central to this is the determination of general - in the sense that they are valid for all admissible values of i and j - expressions for the contributions to K of each of the types of members, i.e., axial, braces, etc. If we let K' be the contribution of a particular type of member to K, then K' may be expressed as

$$K' = L\kappa L^T \qquad \text{(A-1)}$$

where L is an (18r+21)xk transformation matrix, where κ is a diagonal kxk stiffness matrix whose elements are just the axial stiffnesses of the k structural members of the type under consideration, and where T denotes the transpose. Matrix L provides a transformation between the coordinates previously described and a set of coordinates that are parallel to the axes of the structural members being considered; elements of L may be obtained by inspection of the structure, either by observing how a unit force parallel to the axis of a certain member is resolved into forces corresponding to the 18r+21 coordinates or, equivalently, by determining the axial displacement in each member resulting from a unit displacement in one of the coordinates.

Table A-1 gives the cross-sectional area and length of each member; the modulus of elasticity, E, is assumed to be the same for all members.

To illustrate specifically how the stiffness matrix is generated, the formulas for generating L and κ for diagonal members are presented in Appendix B.

Although the L matrix for braces is obtained in the same manner as for other members, special formulas are required for κ, due to the curved nature of these members. It is assumed that the braces (see Figure 2.2) actually comprise five straight pin-connected members each, as shown in Figure A-1. The length and cross-sectional area of the central member are taken as the dimensions $\beta_{i,j}$ and $b_{i,j}$ characteristic of brace $B_{i,j}$.

Table A-1

Type of member	Symbol for member	Cross-sectional area	Length
axial	$A_{i,j}$	$a_{i,j}$	α_j
brace	$B_{i,j}$	$b_{i,j}$*	$\beta_{i,j}$*
circumferential	$C_{i,j}$	$c_{i,j}$	γ
diagonal	$D_{i,j}$	$d_{i,j}$	δ_j
experiment support	E_i	e_i	ε
forward primary mirror support	F_i	f_i	ζ
aft primary mirror support	G_i	g_i	η
secondary mirror support	H_i	h_i	θ

*Since the braces, unlike the other types of members, are not straight and uniform, $b_{i,j}$ and $\beta_{i,j}$ are characteristic rather than actual quantities, as was explained on the preceding page.

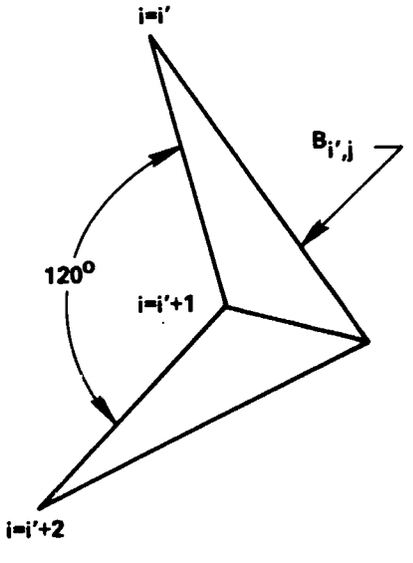

Figure A-1

Assumed brace structure

Since the two members of the brace adjacent to the hexagon must have length γ, $\beta_{i,j}$ is sufficient to determine the lengths of the other three members. Similarly, by specifying that member cross-sectional areas shall be selected to give maximum stiffness/weight ratio, $b_{i,j}$ also becomes sufficient to determine the areas of all five members. In Appendix C formulas dependent only on $b_{i,j}$ and $\beta_{i,j}$ are given for the properties of $B_{i,j}$.

As mentioned in Section 2.1, tangent bars provide compliance between the primary mirror and its three supports. Let a spring with constant k_1 act in a radial direction between the mirror and the first support,* and let a spring with constant k_2 act at the same point in the tangential direction. Likewise, springs with constants k_3 and k_4 act radially and tangentially, respectively, at second support, and springs associated with k_5 and k_6 act at the third support.

We assume that the telescope structure is attached to a spacecraft by means of eighteen springs connected to hexagon j=s. Springs with constants ${}_sk_{3i-2}$, i=1, $\cdots$, 6, act in the axial direction at the six corners of the hexagon; springs with constants ${}_sk_{3i-1}$, i=1, $\cdots$, 6, act vertically; and springs with constants ${}_sk_{3i}$, i=1, $\cdots$, 6, act horizontally.

Mass Matrix

In generating this matrix the mass of the structural members is lumped at the joints by assigning one-half the mass of each member to each of its end points. As this procedure is straightforward, further discussion is unnecessary.

There is, however, a problem related to the mass matrix that warrants comment, and this has to do with the balance of the telescope at its support point, the hexagon j=s. If the telescope is mounted in gimbals, as we have supposed (Section 1.1), rotational isolation of the telescope from the spacecraft depends on how well the telescope is balanced [12]. Assuming that it is balanced about the optical axis, we give formulas below for locating the hexagon j=s such that the telescope is also balanced about a

---

*"First support" is defined on page A-1.

Although (A-2) is approximate, in practice it typically reduces unbalance by four orders of magnitude in a single application, and it should do even better if used iteratively.

Modified Coordinates

Coordinates introduced at the beginning of this appendix are natural and convenient for generation of the stiffness and mass matrices. However, with a view toward reduction of numerical error, the coordinates are modified at this point to yield the significant optical element motions* directly, rather than as linear combinations of the original coordinates. Appendix D gives definitions of the modified coordinates and presents a transformation Q between the two sets of coordinates.

Equations of Motion and the Eigenvalue Problem

Given the symmetric stiffness matrix K, the diagonal positive definite mass matrix M, and the transformation matrix Q, the homogeneous form of the equations of motion,

$$M\ddot{u} + Ku = 0 \qquad \text{(A-4)}$$

in the original coordinates u yield an eigenvalue problem,

$$(-\lambda Q^T MQ + Q^T KQ)v = 0 \qquad \text{(A-5)}$$

in the modified coordinates v. Reference 15 gives a method of solving (A-5) based on Cholesky decomposition of $Q^T MQ$. One may show that $Q^T MQ$ is positive definite [16], as is required for the eigenvalues and eigenvectors to be real.

---

*See Section 3.2.

The eigenvectors ϕ_i and the eigenvalues $\lambda_i = \omega_i^2$ of (A-5) are useful in that they uncouple the equations of motion,

$$Q^T M Q \ddot{v} + Q^T K Q v = Q^T P(t) \qquad \text{(A-6)}$$

where P(t) is a vector of applied loads corresponding to each of the 18r+21 coordinates. The eigenvectors are known as the mode shapes of the structure, and the square roots of the eigenvalues are the corresponding natural frequencies of vibration.

Loads are applied only at the points where the telescope is attached to the spacecraft,* so that (A-6) becomes

$$Q^T M Q \ddot{v} + Q^T K Q v = K_s \xi \qquad \text{(A-7)}$$

where K_s is a matrix comprising the telescope support springs and where ξ is a vector specifying motion of the gimbals (the gimbals are taken to have six degrees of freedom).**

Coordinates Relative to Spacecraft Motion

We desire a telescope whose structural deformation is several orders of magnitude smaller than the motion of the gimbals to which it is attached. Due to our inability to compute mode shapes sufficiently orthogonal to allow extraction of deformation from the total motion, it is necessary to introduce a new set of coordinates that are relative to the gimbal motion rather than relative to an inertial reference frame. Denote by w the new coordinates, which are obtained from

$$w = v - R\xi \qquad \text{(A-8)}$$

---

*Specifically, the telescope is attached to the attitude control gimbals.

**Matrix Q^T is dropped from the right hand side of (A-7) in view of the fact that the part of Q^T associated with the attachment points is just the identity matrix.

Matrix R transforms gimbal motion ξ into equivalent rigid body motion of the telescope structure. That is, if there were no structural deformation (w=0), the total motion of the telescope, v, would be its rigid body motion, $R\xi$.

Substitute (A-8) into (A-7) and recognize that $K_s = Q^T KQR$ to obtain

$$Q^T MQ\ddot{w} + Q^T KQw = -Q^T MQR\ddot{\xi} \qquad \text{(A-9)}$$

Observe that the left hand sides of (A-7) and (A-9) are identical, and thus both have the same frequencies and mode shapes. The two equations differ in that (A-7) is loaded by a few relatively large contact forces, whereas (A-9) is loaded more uniformly by inertia forces at each mass point.

APPENDIX B

Generation of Diagonal Member Contributions to the Stiffness Matrix

Members and Ordering Definitions

There are 12(r-1) diagonal members $D_{i,j}$, organized as follows. For i=1,...,6, $D_{i,j}$ connects joints i,j and $\mu(i+1)$, j+1,* where $\mu(k) = 1 + [(k-1) \bmod 6]$, i.e., $\mu(0) = 6$, $\mu(1) = 1,\ldots, \mu(6) = 6$, $\mu(7) = 1,\ldots$. When i = 7,...,12, $D_{i,j}$ connects joints i, j+1 and $\mu(i+1)$,j. In both cases j=1,...,r-1.

The 12(r-1) diagonal members are assumed to be ordered $D_{1,1}, D_{2,1},\ldots,D_{12,1}, D_{1,2},\ldots, D_{12,r-1}$ in the L and K matrices. The ordering of coordinates is discussed in Appendix A.

The Transformation Matrix L

Since diagonal members involve only the first 18r of the 18r+21 coordinates we let L be (18r) x (12r-12). There are four diagonal members associated with a typical joint of an interior hexagon (j=2,...,r-1), so we consider first $D_{\mu(i-1),j-1}$, which connects joints $\mu(i-1)$,j-1 and i,j. Suppose that $D_{\mu(i-1),j-1}$ is in tension, exerting a unit force on joint i,j. The axial component is $\alpha_{j-1}/\delta_{j-1}$, the vertical component is $-\left(\gamma/\delta_{j-1}\right) \cos i\pi/3$, and the horizontal component is $-\left(\gamma/\delta_{j-1}\right) \sin i\pi/3$. These three components respectively correspond to coordinates ℓ+1, ℓ+2, and ℓ+3, where $\ell = 18(j-1) + 3(i-1)$. Thus we have the three elements of L associated with $D_{\mu(i-1),j-1}$, the $\mu(i-1) + 12(j-2)$ th diagonal member according to the ordering convention:

---

*See Figure 2.1.

$$L_{\ell+1,\ \mu(i-1)+12(j-2)} = \frac{\alpha_{j-1}}{\delta_{j-1}}$$

$$L_{\ell+2,\ \mu(i-1)+12(j-2)} = \frac{-\gamma}{\delta_{j-1}} \cos\frac{i\pi}{3}$$

$$L_{\ell+3,\ \mu(i-1)+12(j-2)} = \frac{-\gamma}{\delta_{j-1}} \sin\frac{i\pi}{3}$$

These elements are evaluated for i=1,...,6, j=2,...,r.

Next consider $D_{i+6,j-1}$, which connects joint $\mu(i+1),j-1$ with i,j and which is the i+6+12(j-2) th diagonal member.

The associated elements of L are

$$L_{\ell+1,\ i+6+12(j-2)} = \frac{\alpha_{j-1}}{\delta_{j-1}}$$

$$L_{\ell+2,\ i+6+12(j-2)} = -\frac{\gamma}{\delta_{j-1}} \sin\frac{(2i-1)\pi}{6}$$

$$L_{\ell+3,\ i+6+12(j-2)} = \frac{\gamma}{\delta_{j-1}} \cos\frac{(2i-1)\pi}{6}$$

where again i=1,...,6 and j=2,...,r.

Diagonal $D_{\mu(i-1)+6,j}$, the $\mu(i-1)+6+12(j-1)$ th diagonal member, connects joint $\mu(i-1),j+1$ with i,j; associated elements of L are

$$L_{\ell+1,\ \mu(i-1)+6+12(j-1)} = -\frac{\alpha_j}{\delta_j}$$

$$L_{\ell+2,\ \mu(i-1)+6+12(j-1)} = -\frac{\gamma}{\delta_j}\cos\frac{i\pi}{3}$$

$$L_{\ell+3,\ \mu(i-1)+6+12(j-1)} = -\frac{\gamma}{\delta_j}\sin\frac{i\pi}{3}$$

where i=1,...,6, but j=1,...,r-1.

Lastly, $D_{i,j}$, the i+12(j-1) th member, which connects joint $\mu(i+1),j+1$ with joint i,j, results in elements

$$L_{\ell+1,\ i+12(j-1)} = -\frac{\alpha_j}{\delta_j}$$

$$L_{\ell+2,\ i+12(j-1)} = -\frac{\gamma}{\delta_j}\sin\frac{(2i-1)\pi}{6}$$

$$L_{\ell+3,\ i+12(j-1)} = \frac{\gamma}{\delta_j}\cos\frac{(2i-1)\pi}{6}$$

which are evaluated for i=1,...,6, j=1,...,r-1.

The Stiffness Matrix κ

This is a (12r-12) x (12r-12) diagonal matrix, the elements of which are the axial stiffnesses of the 12(r-1) diagonal members,

$$\kappa_{i+12(j-1),i+12(j-1)} = \frac{d_{i,j}E}{\delta_j}$$

$d_{i,j}$ being the cross sectional area of $D_{i,j}$ and E being the modulus of elasticity.

APPENDIX C

Optimal Brace Design

We present formulas here for the optimal - in the sense that stiffness/weight ratio is maximized - design of the five member brace described in Appendix A. It is assumed that the structure is pin-connected and that loads are applied only at the ends of the brace, as shown in Figure C-1.

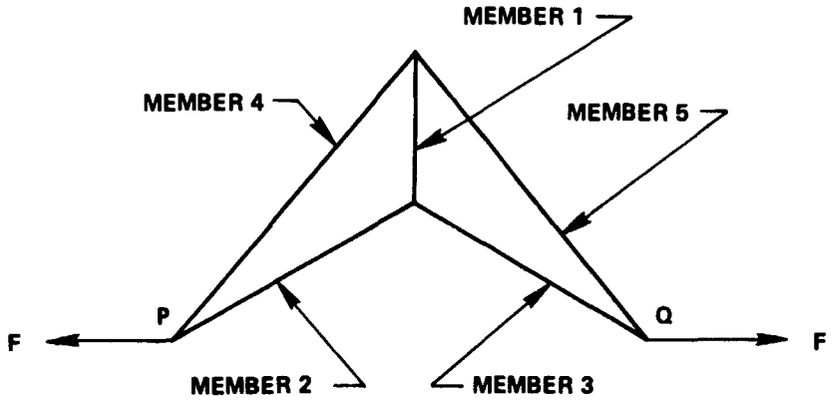

Figure C-1
Brace showing applied loads F

As stated in Appendix A, member 1 has length β and cross-sectional area b (subscripts omitted here), and members 2 and 3 both have length γ.

Let members 2 and 3 have cross-sectional area A_1, and let members 4 and 5 have length ℓ and area A_2.

The stiffness of the brace (in the direction of F) is

$$K = 3\beta^2 bE\left[\left(\frac{2\gamma b}{A_1} + \beta\right)\left(2\beta + \gamma\right)^2 + \frac{2\ell^3 b}{A_2}\right]^{-1}$$

where

$$\ell = \sqrt{\gamma^2 + \gamma\beta + \beta^2}$$

and where E is the modulus of elasticity. If ρg is the weight density, the brace has weight

$$W = \rho g(\beta b + 2\gamma A_1 + 2\ell A_2)$$

For an optimal brace

$$A_1 = b$$

$$A_2 = \frac{b\ell}{2\beta+\gamma}$$

and it follows that

$$K = \frac{3bE}{(\gamma+2\beta)\left[4\left(\frac{\gamma}{\beta}\right)^2 + 7\,\frac{\gamma}{\beta} + 4\right]}$$

$$W = \frac{\rho g \beta^2 b}{\gamma+2\beta}\left[4\left(\frac{\gamma}{\beta}\right)^2 + 7\,\frac{\gamma}{\beta} + 4\right]$$

One can see that K/W is independent of b, but it is possible to choose optimal value of β. We have

$$\frac{K}{W} = \frac{3E}{\rho g \beta^2}\left[4\left(\frac{\gamma}{\beta}\right)^2 + 7\,\frac{\gamma}{\beta} + 4\right]^{-2}$$

which is largest when $\beta = \gamma$. However, since $\beta = \gamma$ would result in a structure twice as large as the basic hexagon, it may be

desirable to use a smaller value of β, a possibility that we now examine. Imagine that the brace is replaced by a single straight rod connecting points P and Q in Figure C-1. The stiffness/weight ratio of the rod is

$$\frac{K'}{W'} = \frac{E}{3\rho g \gamma^2}$$

and

$$R = \left(\frac{K}{W}\right) \Big/ \left(\frac{K'}{W'}\right) = 9\left(4\,\frac{\gamma}{\beta} + 7 + 4\,\frac{\beta}{\gamma}\right)^{-2}$$

R may be thought of as the structural efficiency of the brace, and Figure C-2 shows the dependence of R on β/γ.

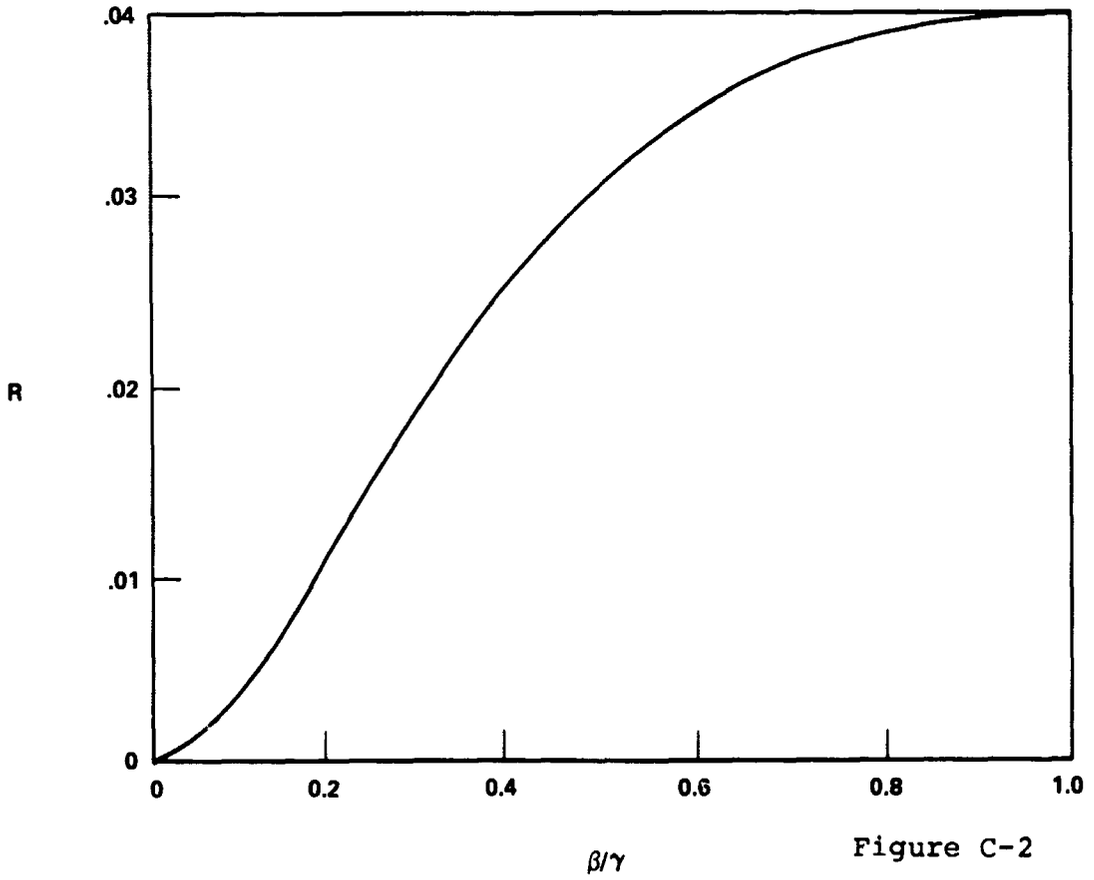

Figure C-2

Brace structural efficiency vs. central member length

APPENDIX D

Transformation Between Modified and Original Coordinates

Let u_k, k = 1,..., 18r + 21 denote coordinates defined in Appendix A, and let v_k, k = 1,..., 18r + 21 denote modified coordinates that differ from the respective u_k only as noted below.

$v_{18r + 4}$: x translation of the center of the primary mirror.

$v_{18r + 7}$: rotation of the primary about y.

$v_{18r + 10}$: rotation of the primary about z.

$v_{18r + 16}$: x translation of the secondary mirror relative to the primary.

$v_{18r + 17}$: y translation of the secondary relative to the primary.

$v_{18r + 18}$: z translation of the secondary relative to the primary.

$v_{18r + 20}$: rotation about y of the secondary relative to the primary.

$v_{18r + 21}$: rotation about z of the secondary relative to the primary.

The (18r + 21) x (18r + 21) transformation matrix Q, u = Qv, is defined by

$$u_{18r+4} = v_{18r+4} + \frac{\ell_f}{2}\left(v_{18r+7} - \sqrt{3}\, y_{18r+10}\right)$$

$$u_{18r+7} = v_{18r+4} + \frac{\ell_f}{2}\left(v_{18r+7} + \sqrt{3}\, y_{18r+10}\right)$$

$$u_{18r+10} = v_{18r+4} - \ell_f\, y_{18r+7}$$

$$u_{18r+16} = v_{18r+4} + v_{18r+16}$$

$$u_{18r+17} = v_{18r+14} + v_{18r+17} + \Sigma\alpha\, v_{18r+10}$$

$$u_{18r+18} = v_{18r+15} + v_{18r+18} - \Sigma\alpha\, v_{18r+7}$$

$$u_{18r+20} = v_{18r+7} + v_{18r+20}$$

$$u_{18r+21} = v_{18r+10} + v_{18r+21}$$

$u_k = v_k$ for remaining values of k

where ℓ_f is the radial distance to the primary mirror supports and where $\Sigma\alpha$ is the distance between the mirrors,

$$\Sigma\alpha = \frac{\alpha_1}{2} + \alpha_2 + \ldots + \alpha_{r-2}$$

APPENDIX E

Computer Program Flowchart

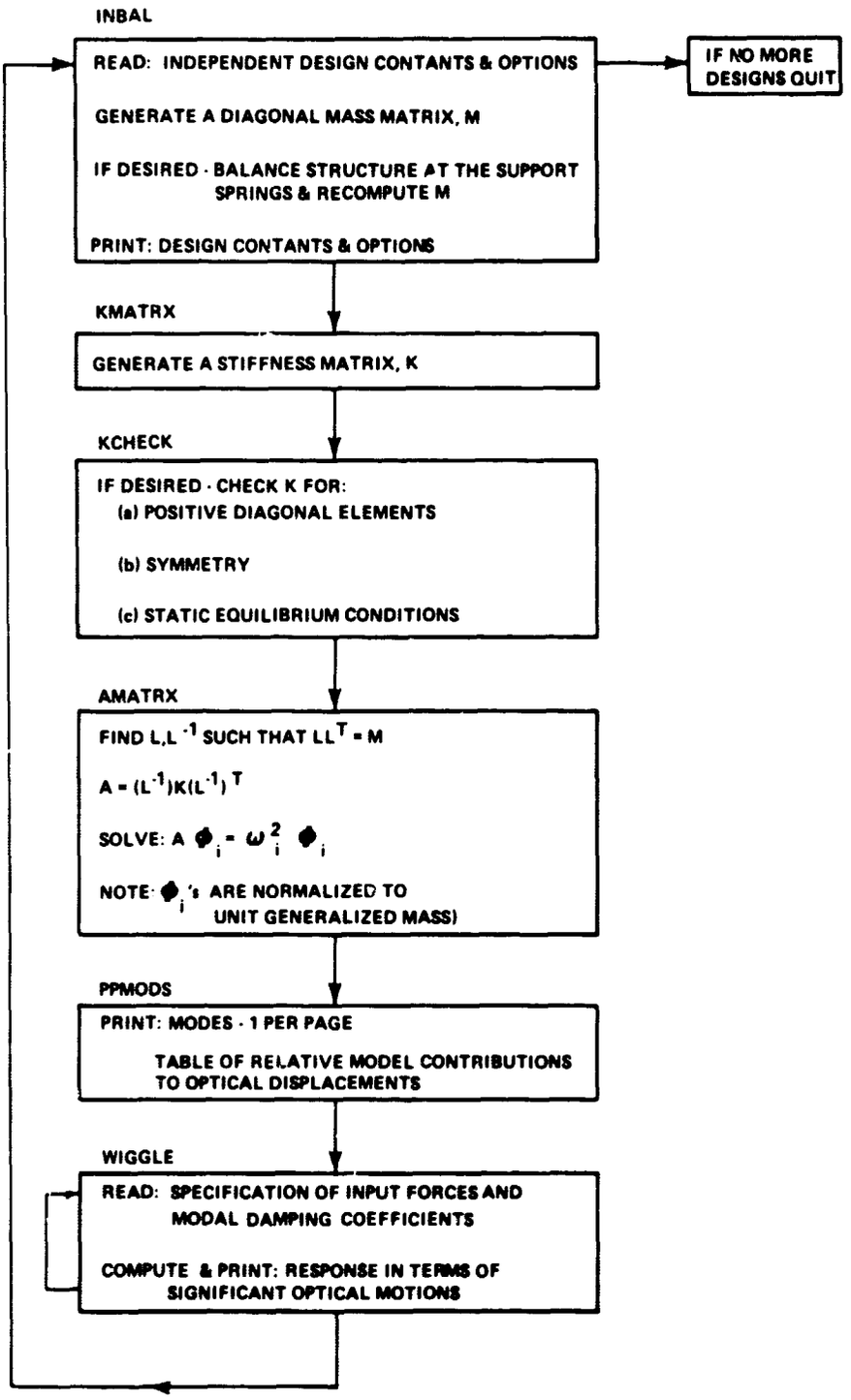

APPENDIX F

Constants Relating to the 1 Meter, f-30 Design

(All symbols used are defined in Section 2.1 and Appendix A.)

Lengths (inches)

j =	1	2	3	4	5	6
α_j =	10.	34.	34.	56.61	10.49	12.

$\beta_{ij} = 6.,\ i=1,\ldots,6,\ j=1,\ldots,7$

$\gamma = 24.25$

$\varepsilon = 25.54$

$\zeta = 14.15$

$\eta = 18.56$

$\theta = 21.83$

Areas (inch^2)

$$a_{ij} = \begin{cases} 0.25, & i = 2,3,5,6, \quad j=1,\ldots,6 \\ 0.275, & i = 1,4, \quad j=1,\ldots,6 \end{cases}$$

$$b_{ij} = .05, \quad i = 1,\ldots,6, \quad j=1,\ldots,7$$

$$c_{ij} = \begin{cases} 0.25, & i = 1,\ldots,6, \quad j=1,2 \\ 0.1, & i = 1,\ldots,6, \quad j=3,4,5 \\ 0.25, & i = 1,3,5, \quad j=6,7 \\ 0.1, & i = 2,4,6, \quad j=6,7 \end{cases}$$

$$d_{ij} = \begin{cases} 0.25, & i = 1,3,4,6,7,9,10,12, \quad j = 1 \\ 0.275, & i = 2,5,8,11, \quad j = 1 \\ .05, & i = 1,3,4,6,7,9,10,12, \quad j = 2,\ldots,5 \\ .055, & i = 2,5,8,11, \quad j = 2,\ldots,5 \\ .05, & i = 1,3,7,9, \quad j = 6 \\ 0.11, & i = 2,8, \quad j = 6 \\ 0.10, & i = 4,6,10,12, \quad j = 6 \\ .055, & i = 5,11, \quad j = 6 \end{cases}$$

$$e_i = \begin{cases} 0.25, & i = 2,3,5,6 \\ 0.275, & i = 1,4 \end{cases}$$

$$f_i = \begin{cases} 0.25, & i = 1,\ldots,4 \\ 0.225, & i = 5,6 \end{cases}$$

$$g_i = \begin{cases} 0.50, & i = 1,\ldots,4 \\ 0.45, & i = 5,6 \end{cases}$$

$$h_i = \begin{cases} 0.25, & i = 2,3,5,6 \\ 0.275, & i = 1,4 \end{cases}$$

Inertias

Mass of primary = 0.83 lb-sec^2/in

Mass of secondary = .065 lb-sec^2/in

Mass of experiments = 1.30 lb-sec^2/in

Axial moment of inertia of primary = 161. in-lb-sec^2

Axial moment of inertia of secondary = 0.292 in-lb-sec^2

Transverse moment of inertia of secondary = 0.146 in-lb-sec^2

Springs

$$k_i = \begin{cases} 3750. \text{ lb/in}, & i = 1,3,5 \text{ (radial)} \\ 6 \times 10^6 \text{ lb/in}, & i = 2,4,6 \text{ (tangential)} \end{cases}$$

$h = 100$ lb

$_sk_i$, $i = 1,\ldots,18$: Computed to give a support stiffness of 1.0% of the stiffness of the structure at the points where the springs are attached.

General

$r = 7, \quad s = 5$

modulus of elasticity of Invar = 21.4×10^6 lb/in^2

density of Invar = 7.49×10^{-4} lb-sec^2/in^4

APPENDIX G

Test for Numerical Accuracy

The response of the structure should depend continuously on parameters of its design. This is a consequence of the fact that differential equation solutions depend continuously on parameters of the equation [18]. Consider rotation of the primary mirror in response to vertical or horizontal translation excitation to be composed of two parts, internal deformation and gross motion, and assume that the former is largely independent of how the structure is supported, whereas the latter depends mostly on how and where it is supported. Now, if several telescope designs differing only in axial location of the support point* are tried on the computer, results should show a continuous dependence of response on support point location, which we denote by α; to the extent that there is scatter in a curve of response vs. α, there is error in the response. Furthermore, when the excitation is vertical or horizontal translation and when the response in question is rotation of the primary mirror, it is possible to determine the relation between α and gross motion of the structure by analysis of an equivalent rigid body model of the telescope. This provides a check on the results that is completely independent of the structural and modal analyses.

Figure G-1 shows a rigid body model of the telescope having two degrees of freedom, vertical translation, denoted

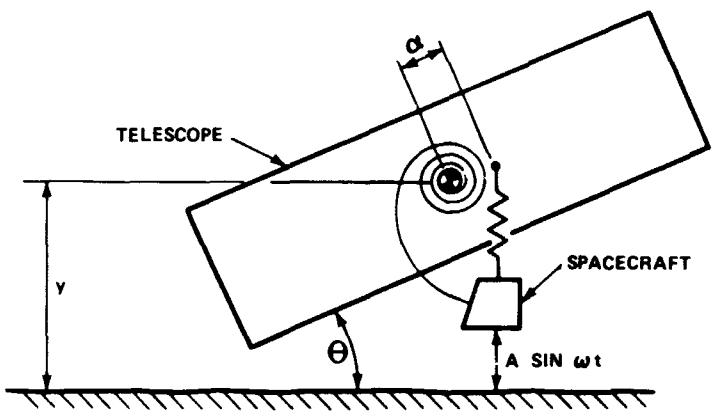

Figure G-1
Rigid body model

*That is, different sets of values for α_4 and α_5 but with the sum $\alpha_4 + \alpha_5$ remaining constant.

by y, and rotation, denoted by θ. The telescope has mass m and moment of inertia I, and it is mounted to the spacecraft by means of a translational spring with constant k_y and a rotational spring with constant k_θ. The spacecraft has vertical sinusoidal motion with amplitude A and frequency ω. From the equations of motion one can show that

$$\theta = C_1 \alpha \sin\omega t \tag{G-1}$$

where C_1 may be obtained from

$$C_1 = \frac{-m\omega^2 k_y A}{k_y k_\theta - I\omega^2 k_y - m\omega^2 k_\theta + Im\omega^4} \tag{G-2}$$

when $\alpha^2 << k_\theta/k_y$, as is normally the case.

In line with the assumption stated earlier, it is postulated that primary mirror rotation, ϕ, depends on α as follows:*

$$\phi = \left\{ \left[(C_1 \alpha/\sqrt{2}) + C_2 \right]^2 + C_3^2 \right\}^{1/2} \tag{G-3}$$

Constants C_2 and C_3 represent rotations about the two axes normal to the optical axis, these rotations being attributable to deformation of the telescope rather than to its gross motion.

The program is tested by running ten designs that differ only in support point location, α. Changes in α between designs are kept small, but since this one parameter is fundamental to both the mass and stiffness matrices, error accumulates differently in each design. To evaluate the results of the ten

---

*The $\sqrt{2}$ appears because C_1 represents amplitude, whereas the other quantities represent rms values.

designs mirror rotation ϕ is plotted against α, C_1 is obtained from (G-2), and C_2 and C_3 are obtained from a least squares fit of (G-3) to the ten points.

Figures G-2 through G-5 illustrate results for both the 1 meter f-30 and the 2 meter f-60 designs and for excitation in both the vertical and horizontal directions. The ten designs yield the ten points in the figures and the lines are the least squares fits. The first two plots illustrate especially well both the accuracy of the program and the accuracy with which slope C_1 can be predicted from a simple rigid body model. The last two plots illustrate better than the first two the validity of functional form (G-3).

A further observation should be made. It has been shown that for a rigid telescope pointing error is minimized when the mass center and the support point coincide [2]. But for a flexible telescope, primary mirror rotation, which is among the most important of the significant motions, is minimal for some nonzero α. If this nonzero value of α should remain substantially fixed for the various excitations expected in service, then pointing performance of a flexible telescope might be improved by picking α properly.

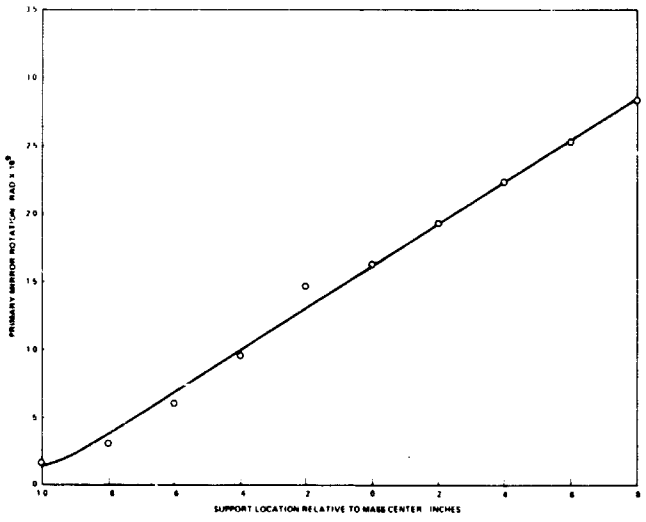

Figure G-2
1 meter f-30 design
Response to vertical translation

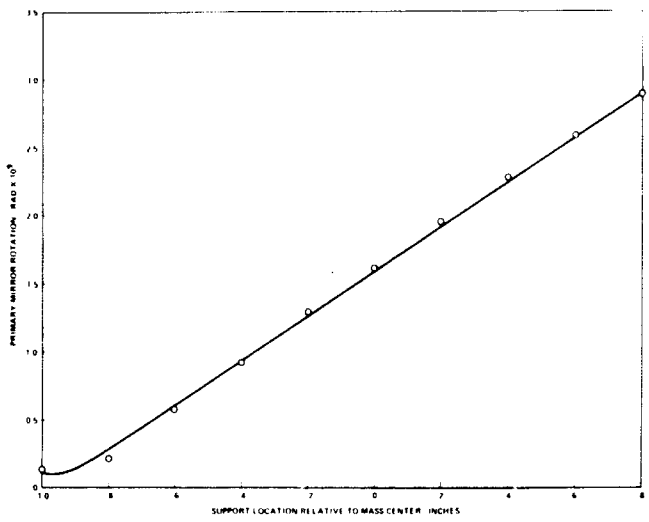

Figure G-3
1 meter f-30 design
Response to horizontal translation

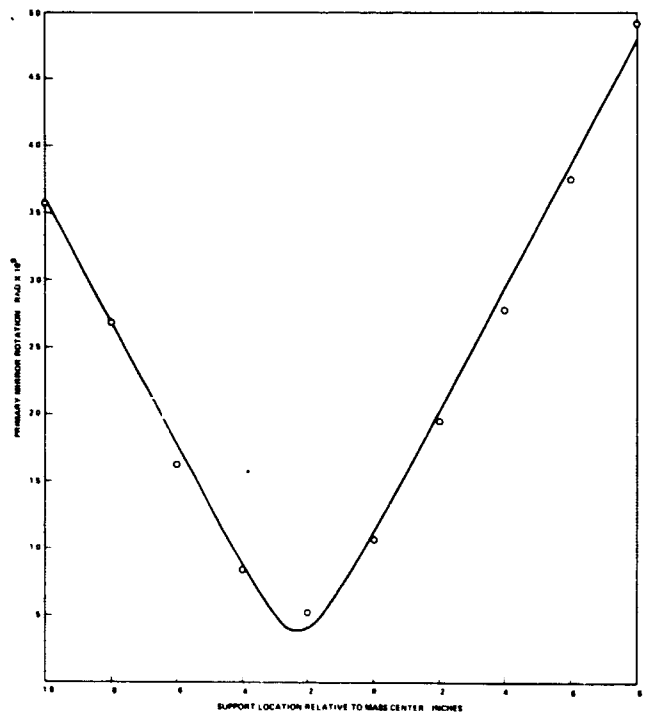

Figure G-4
2 meter f-60 design
Response to vertical translation

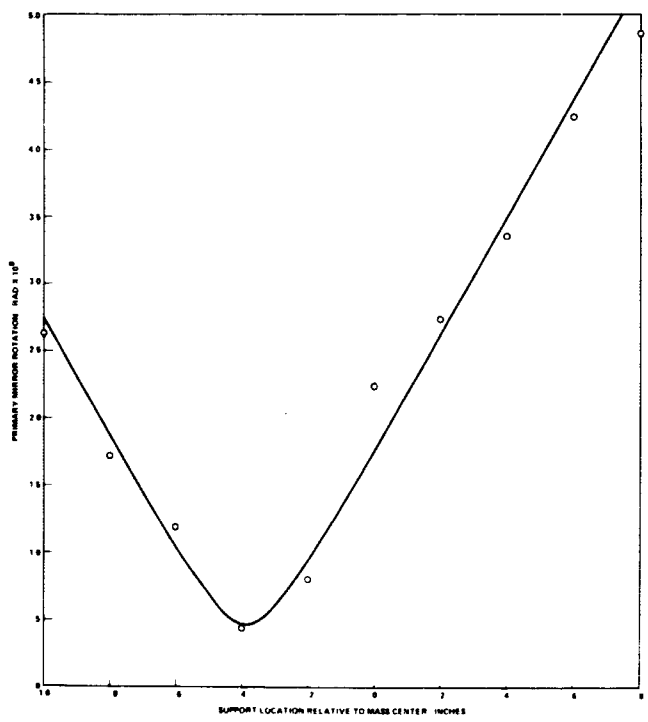

Figure G-5
2 meter f-60 design
Response to horizontal translation

REFERENCES

1. Wood, D. B., "The Use of Manned Space Flight for Astronomy," Bellcomm TM-69-1015-1, February 5, 1969.

2. Smith, P. G., "The Pointing Accuracy of an Orbiting Gimbal Mounted Telescope," Bellcomm TM-69-1022-2, February 17, 1969.

3. Elrod, B. D., and Kranton, J., "Crew Motion Considerations for Hard vs. Gimbal Mounting of ATM Experiments, Bellcomm TM-66-1022-3, December 23, 1966.

4. "Single Axis Gimbaled ATM Control System Study," Martin Marietta (Denver) ED-2002-81, April 6, 1967.

5. Morrell, F. R., "Precise Attitude Stabilization of a Large Orbiting Telescope Coupled to a Crew Compartment," IEEE Trans. Aerospace and Electronic Systems, March 1969, pp. 294-299.

6. Smith, P. G., "A Mathematical Model for Simulation of the Apollo Telescope Mount Pointing Control System," Bellcomm TR-68-620-1, May 8, 1969, p. 4.

7. Mu, H. H. and Garba, J. A., "Photoheliograph Structural Development," JPL Report 750-19, March 15, 1969.

8. Anderson, G. M., "Dynamic Distortion of a Gimbaled Telescope," Bellcomm TM-69-1022-3, May 21, 1969.

9. Kimery, R. P., "Analysis of Spar Bending Modes," Sperry Rand Space Support Division SP-231-0175, January 31, 1969.

10. Personal communication, J. A. Power (MSFC), May 5, 1969.

11. "Final Report: Optical Astronomy Package Feasibility Study for Apollo Applications Program," Vol. II, Part E, Kollsman Instrument Corporation, Space Division, March 1966, p. 16, Figure 2.7.

12. Reference 2, p. 35.

13. Reference 2, p. 29.

14. "Crew Motion Data Analysis," Apollo Applications Program Payload Integration Technical Report No. ED-2002-644, Martin Marietta Corporation, October 14, 1968.

15. Hou, S. N., "300 Degree of Freedom Modal Analysis Program 'MAP' for Structural Dynamics - Case 320," Bellcomm Memorandum for File, to be published.

16. Finkbeiner, D. T., Introduction to Matrices and Linear Transformations, W. H. Freeman and Co., 1960, Theorem 9.25.

17. Brewer, F. A., "Computer Program Writeup for MODES - AAP Telescope Vibration Study Program - Case 620," Bellcomm Memorandum for File, to be published.

18. Coddington, E. A. and Levinson, N., Theory of Ordinary Differential Equations, McGraw-Hill, 1955, Theorem 7.4.

END

DATE

FILMED

AUG 6 1970